Supporting Information **for**

High-quality all-inorganic $CsPbBr_3$ single crystals prepared by a facile one-step solution growth method

Mingming Chen[a, b], Youwen Yuan[b], Yuan Liu[b], Dawei Cao[*b], and Chunxiang Xu[*a]

[1] State Key Laboratory of Bioelectronics, School of Biological Science and Medical Engineering, Southeast University, Nanjing, Jiangsu 210096, China

[2] Department of Physics, School of Physics and Electronic Engineering, Jiangsu University, Zhenjiang, Jiangsu 212013, China

*** Corresponding Authors**

E-mail: dwcao@ujs.edu.cn (D. Cao); xcxseu@seu.edu.cn (C. Xu)

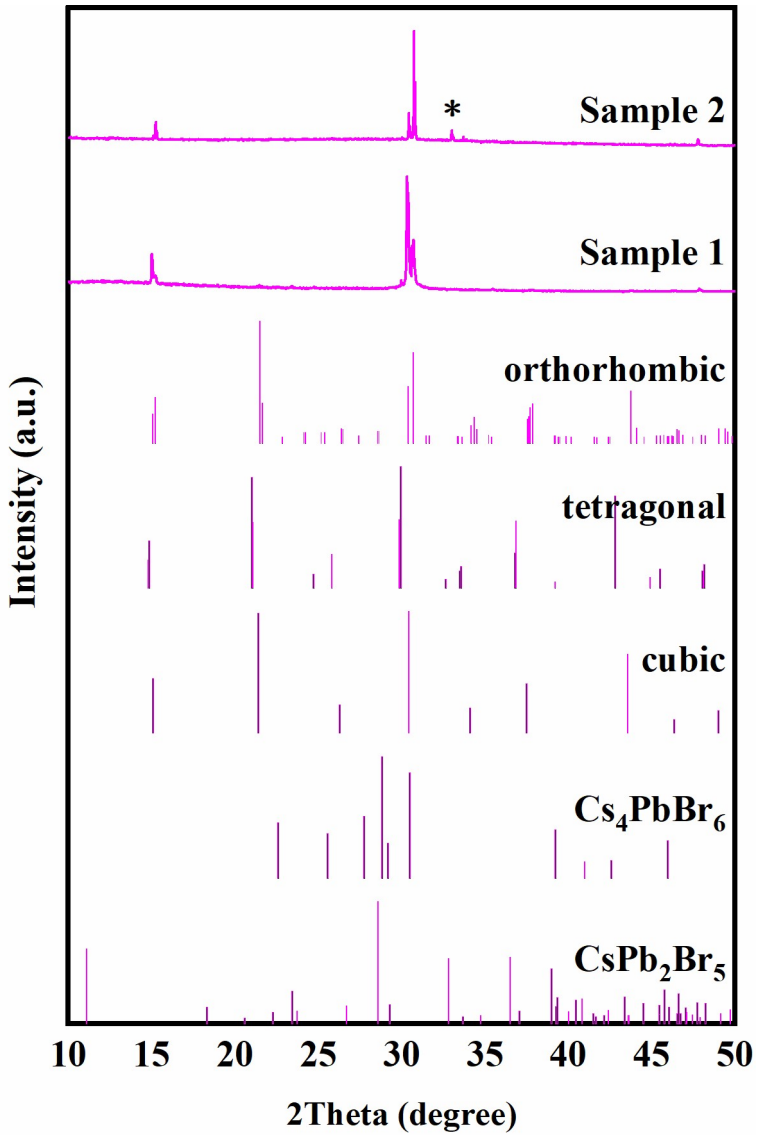

Figure S1. Powder XRD patterns of the as-grown $CsPbBr_3$ single crystal (**Sample 1**), *HPS* grown $CsPbBr_3$ single crystal (**Sample 2**), orthorhombic $CsPbBr_3$, tetragonal $CsPbBr_3$, cubic $CsPbBr_3$, Cs_4PbBr_6, and $CsPbBr_5$. The diffraction peak (labeled as *) in **Sample 2** is related to (310) of $CsPb_2Br_5$.

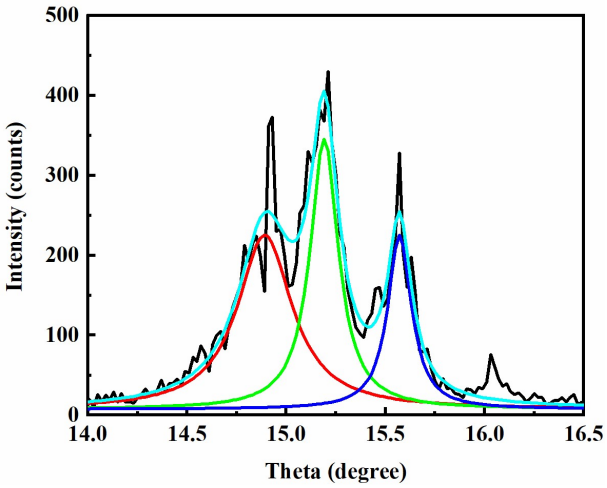

Figure S2. High-resolution XRD rocking curve spectrum (black) of $CsPbBr_3$ single crystals prepared using *HPS* method. The XRD rocking curve spectrum was fitted using the Lorentz function (shown in red, green, blue, and cyan lines). Here, the multi-diffraction peaks may be caused by complex multi-phase ($CsPbBr_3$/$CsPb_2Br_5$) of the sample, in which the peak at 15.09° is assigned to (002) of $CsPbBr_3$.

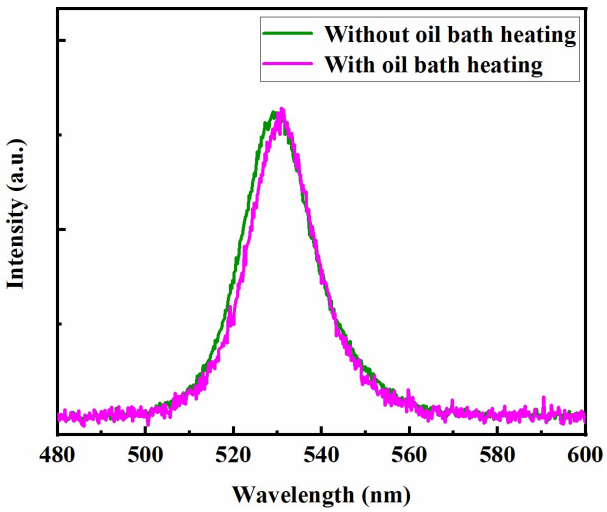

Figure S3. PL spectra of $CsPbBr_3$ single crystals prepared with and without oil bath heating.

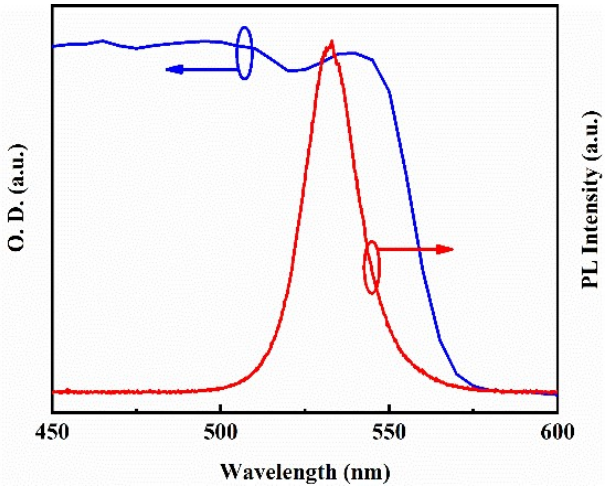

Figure S4. PL and absorption spectra of $CsPbBr_3$ single crystal.

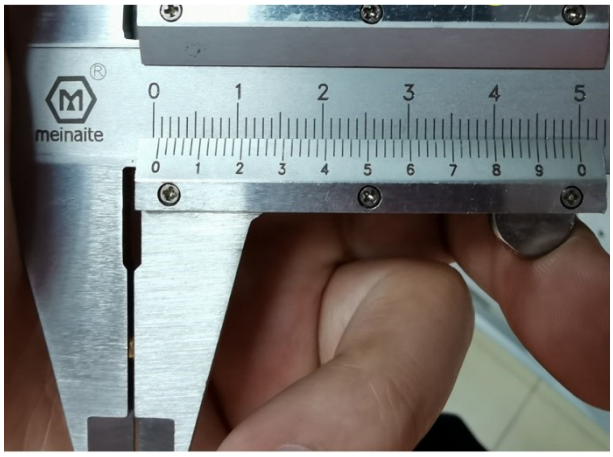

Figure S5. The thickness of the selected $CsPbBr_3$ single crystals for *I-V* measurements.

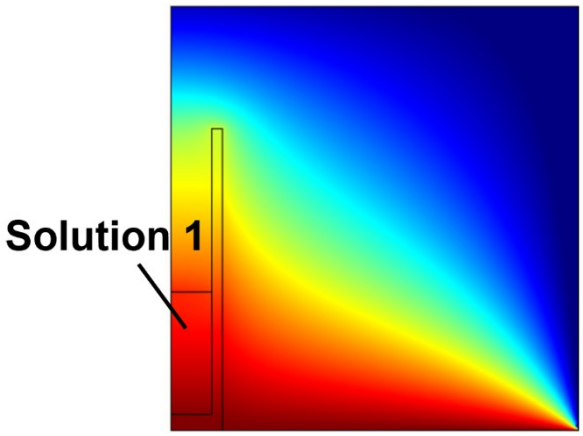

Figure S6. Calculated steady-state temperature field distribution of the precursor solution (labeled as solution 1) heated on the hot table.

Table S1. Comparison of trap density of $CsPbBr_3$ single crystal reported in this work and related results reported previously.

Material	Method	Trap density (cm^{-3})	Reference
$CsPbBr_3$	Inverse temperature crystallization	1.1×10^{10}	1
$CsPbBr_3$	Bridgman	1.9×10^{9}	2
$CsPbBr_3$	Bridgman	6.3×10^{10}	3
$CsPbBr_3$	Antisolvent vapor	2.8×10^{10}	4
$CsPbBr_3$	Low-temperature crystallization in water	1.7×10^{10}	5
$CsPbBr_3$	Inverse temperature crystallization	7.6×10^{10}	5
$CH_3NH_3PbBr_3$	seed-induced heterogeneous nucleation	2.6×10^{10}	6
$CH_3NH_3PbBr_3$	cavitation-triggered asymmetric crystallization	$\sim 10^{11}$	7
$CH_3NH_3PbI_3$	Inverse temperature crystallization with ligand regulation	7×10^{10}	8
$CH_3NH_3PbBr_3$	liquid-diffused separation induced crystallization	4.4×10^{9}	9
$CH_3NH_3PbI_3$	Inverse temperature crystallization	1.4×10^{10}	10
$CH_3NH_3PbBr_3$	Inverse temperature crystallization	3×10^{10}	10
$CsPbBr_3$	HPS with an oil bath heating	5.1×10^{9}	This work

Reference

1. Saidaminov, M. I.; Haque, M. A.; Almutlaq, J.; Sarmah, S.; Miao, X.; Begum, R.; Zhumekenov, A. A.; Dursun, I.; Cho, N.; Murali, B.; Mohammed, O. F.; Wu, T.; Bakr, O. M., Inorganic Lead Halide Perovskite Single Crystals: Phase-Selective Low-Temperature Growth, Carrier Transport Properties, and Self-Powered Photodetection. *Adv. Opt. Mater.* **2017,** *5* (2), 1600704.

2. Song, J.; Cui, Q.; Li, J.; Xu, J.; Wang, Y.; Xu, L.; Xue, J.; Dong, Y.; Tian, T.; Sun, H.; Zeng, H., Ultralarge All-Inorganic Perovskite Bulk Single Crystal for High-Performance Visible–Infrared Dual-Modal Photodetectors. *Adv. Opt. Mater.* **2017,** *5* (12), 1700157.

3. Zhang, P.; Zhang, G.; Liu, L.; Ju, D.; Zhang, L.; Cheng, K.; Tao, X., Anisotropic Optoelectronic Properties of Melt-Grown Bulk CsPbBr3 Single Crystal. *J. Phys. Chem. Lett.* **2018,** *9* (17), 5040-5046.

4. Miao, X.; Qiu, T.; Zhang, S.; Ma, H.; Hu, Y.; Bai, F.; Wu, Z., Air-stable CsPb1−xBixBr3 ($0 \leq x \ll 1$) perovskite crystals: optoelectronic and photostriction properties. *J. Mater. Chem. C* **2017,** *5* (20), 4931-4939.

5. Peng, J.; Xia, C. Q.; Xu, Y.; Li, R.; Cui, L.; Clegg, J. K.; Herz, L. M.; Johnston, M. B.; Lin, Q., Crystallization of CsPbBr3 single crystals in water for X-ray detection. *Nat. Commun.* **2021,** *12* (1), 1531.

6. Liu, Y.; Yang, Z.; Cui, D.; Ren, X.; Sun, J.; Liu, X.; Zhang, J.; Wei, Q.; Fan, H.; Yu, F.; Zhang, X.; Zhao, C.; Liu, S., Two-Inch-Sized Perovskite CH3NH3PbX3 (X = Cl, Br, I) Crystals: Growth and Characterization. *Adv. Mater.* **2015,** *27* (35), 5176-5183.

7. Peng, W.; Wang, L.; Murali, B.; Ho, K.; Bera, A.; Cho, N.; Kang, C.; Burlakov, V. M.; Pan, J.; Sinatra, L.; Ma, C.; Xu, W.; Shi, D.; Alarousu, E.; Goriely, A.; He, J.; Mohammed, O. F.; Wu, T.; Bakr, O. M., Solution-Grown Monocrystalline Hybrid Perovskite Films for Hole-Transporter-Free Solar Cells. *Adv. Mater.* **2016,** *28* (17), 3383-3390.

8. Liu, Y.; Zheng, X.; Fang, Y.; Zhou, Y.; Ni, Z.; Xiao, X.; Chen, S.; Huang, J., Ligand assisted growth of perovskite single crystals with low defect density. *Nat. Commun.* **2021,** *12* (1), 1686.

9. Yao, F.; Peng, J.; Li, R.; Li, W.; Gui, P.; Li, B.; Liu, C.; Tao, C.; Lin, Q.; Fang, G., Room-temperature liquid diffused separation induced crystallization for high-quality perovskite single crystals. *Nat. Commun.* **2020,** *11* (1), 1194.

10. Saidaminov, M. I.; Abdelhady, A. L.; Murali, B.; Alarousu, E.; Burlakov, V. M.; Peng, W.; Dursun, I.; Wang, L.; He, Y.; Maculan, G.; Goriely, A.; Wu, T.; Mohammed, O. F.; Bakr, O. M., High-quality bulk hybrid perovskite single crystals within minutes by inverse temperature crystallization. *Nat. Commun.* **2015,** *6* (1), 7586.